Discretization effects and the influence of walking speed in cellular automata models for pedestrian dynamics

Ansgar Kirchner[1,2,5], **Hubert Klüpfel**[2,3],
Katsuhiro Nishinari[1,4], **Andreas Schadschneider**[1,6] **and**
Michael Schreckenberg[2]

[1] Institut für Theoretische Physik, Universität zu Köln, 50923 Köln, Germany
[2] Physik von Transport und Verkehr, Universität Duisburg-Essen,
47048 Duisburg, Germany
[3] TraffGo GmbH, Falkstraße 73-77, 47058 Duisburg, Germany
[4] Department of Applied Mathematics and Informatics, Ryukoku University,
Shiga, Japan
E-mail: aki@thp.uni-koeln.de, kluepfel@traffgo.com, knishi@rins.ryukoku.ac.jp,
as@thp.uni-koeln.de and schreckenberg@uni-duisburg.de

Abstract. We study discretization effects in cellular automata models for
pedestrian dynamics by reducing the cell size. Then a particle occupies more
than one cell which leads to subtle effects in the dynamics, e.g. non-local conflict
situations. Results from computer simulations of the floor field model are
compared with empirical findings. Furthermore, the influence of increasing the
maximal walking speed v_{max} is investigated by increasing the interaction range
beyond nearest neighbour interactions. The extension of the model to $v_{max} > 1$
turns out to be a severe challenge which can be solved in different ways. Four
major variants are discussed that take into account different dynamical aspects.
The variation of v_{max} has a strong influence on the shape of the flow–density
relation. We show that walking speeds $v_{max} > 1$ lead to results which are in very
good agreement with empirical data.

Keywords: cellular automata, driven diffusive systems (theory), stochastic
processes, traffic and crowd dynamics

[5] Present address: BERATA GmbH, Geschäftsstelle Hamburg, Nagelsweg 24, 20097 Hamburg, Germany.

[6] Author to whom any correspondence should be addressed.

Contents

1. Introduction

The understanding of the dynamical features of pedestrian dynamics has been the aim of many investigations over the last few years [1]–[3]. Recently approaches based on cellular automata (CA) have also been suggested. CA models are discrete in space, time and state variables. On the one hand, this makes the models ideally suited for large scale computer simulations. On the other hand, the discreteness has to be regarded as an approximation of reality. In this paper we want to investigate some more fundamental questions related to general aspects of physical modelling using discrete models. More specifically, we try to elucidate the qualitative and, in some cases, even quantitative influence of the parameters related to the discretization. As with any other kind of simulation (e.g. fluid dynamics [4]), two major decisions have to be made for the description to be used: macroscopic versus microscopic and discrete versus continuous [5]. Although we do not consider it explicitly here, taking the continuum limit of the discrete models would contribute to a better understanding of their relation to continuous models.

As we will see, the discreteness leads to some problems that will be exemplified using the so-called floor field CA model that has been introduced in [6]–[8]. The big advantage of this model compared to other CA approaches for pedestrian dynamics [9]–[13] is that the floor field model is able to reproduce most of the characteristic aspects of pedestrian

dynamics, especially the different collective effects observed empirically [1, 2, 14, 15]. Here, the inclusion of friction effects allows us to describe many important observations, especially in egress and evacuation scenarios [8, 16].

There are three foremost basic parameters that any CA model is based on: the interaction range, which in traffic models [17] is usually given by the maximal velocity v_{max}, the timescale Δt and the generic length scale a, corresponding to the size of one grid cell. The variation of Δt will only cause the rescaling of all time values such as averaged evacuation times and is therefore, from a theoretical point of view, not very interesting. In contrast, variations of v_{max} and a will turn out to have a strong qualitative influence on the *dynamical* properties of the model.

The outline of the paper is as follows. First, we present extensions of the basic model (with $v_{max} = 1$) to larger interaction ranges $v_{max} > 1$. Four possible variants of the extension are considered, based on different aspects of the dynamics, especially the treatment of crossing paths. Monte Carlo simulations will be presented and compared to empirical data. Then we investigate the effects of a reduction of the length scale a. We will also show that a finer spatial discretization (by reducing a from $a = 40$ to 20 cm) has strong effects on the dynamics.

But first, we will review the most important characteristics of the basic model with $v_{max} = 1$ and $a = 40$ cm in the next section.

2. Cellular automata models

For pedestrian dynamics, in a natural spatial discretization one introduces cells of 40 cm × 40 cm. This corresponds to the typical space occupied by a person in a dense crowd. Therefore, each cell can then either be empty or occupied by (at most) one pedestrian (hard core exclusion).

Most CA approaches use a parallel (synchronous) update where the dynamical rules $\mathcal{Z}$ have to be applied to all particles at the same time. This introduces a timescale Δt. In stochastic CA models the motion to other cells at each discrete time step $t \to t + \Delta t$ is controlled by transition probabilities. In the simplest case, which is used most often, each pedestrian is allowed to move only to one of his/her four nearest neighbour cells.

The effects of the discretization and interaction range that we want to investigate here will appear in any CA model. However, our testing ground will be a specific CA, namely the floor field model. It can be regarded as a two-dimensional generalization of the asymmetric simple exclusion process (ASEP) (see e.g. [18, 19]) where the transition probabilities are determined *dynamically* through a coupling to so-called *floor fields* [6, 7]. In turn, these floor fields are changed by the motion of the pedestrians which leads to feedback effects. This way of implementing the interactions is inspired by the form of communication in insect societies (e.g. ants) and the interaction can be described as *virtual chemotaxis*. Generically a movement in the direction of larger fields is preferred. The key point is that an interaction that is long ranged in space can be translated into a local interaction, but with 'memory'. Note that in contrast to chemotaxis and trail formation [20]–[23] in our model the trace is only virtual, i.e. cannot be observed empirically. We do not give a full definition and discussion of the floor field model, which can be found in [6]–[8], [24, 25], but focus on the aspects that are important in the following.

The floor field consists of two parts, a static and a dynamic field. Both are discrete and we can imagine the field strength as the number of virtual pheromones present at a site. The fixed *static floor field S* is not changed by the presence of the pedestrians. S is used to specify regions of space which are more attractive, e.g. exits or shop windows. In case of an evacuation simulation the static floor field S describes the shortest distance to the closest exit door measured in steps, i.e. the number of lattice sites to the exit [7]. Steps can be carried out to the four next neighbour sites. The field values increase towards the door.

Collective effects such as lane formation and herding [1, 2, 26, 27] that are based on a long range interaction between pedestrians can be taken into account via a dynamically varying floor field D [6]. The *dynamic floor field D* is a virtual trace left by the pedestrians and has its own dynamics, i.e. diffusion and decay. It is used to model different forms of interaction between the pedestrians. At $t = 0$ the dynamic field is set to zero for all sites (x, y) of the lattice, i.e. $D_{xy} = 0$. Whenever a particle jumps from site (x, y) to one of the four neighbouring cells, D at the origin cell is increased by one: $D_{xy} \rightarrow D_{xy} + 1$. Furthermore, the dynamic floor field is time dependent; it has diffusion and decay controlled by two parameters $0 \leq \alpha, \delta \leq 1$, which leads to broadening and dilution of the trace [6].

The coupling of the particles to the static and dynamic floor field is controlled by coupling constants k_S and k_D, respectively. A strong coupling to the static field implies an almost deterministic motion in the direction of larger fields. On the other hand, if the coupling to the dynamic field dominates, herding effects become important, where pedestrians blindly follow others as may happen in the case of panic.

An important extension that makes the dynamics more realistic is the concept of *friction* [8, 16]. It has been implemented in other models in a direct way as contact friction [27]. However, in our approach it concerns the behaviour of two (or more) pedestrians that try to move to the same cell. With some probability μ, called the friction parameter, none of the particles is allowed to move, whereas with probability $1 - \mu$ one of the particles is chosen randomly to occupy the target cell. This leads to effects similar to arching in granular materials [27, 28].

3. Extensions to $v_{\mathrm{max}} > 1$

In the definition of the model given above, particles are only allowed to move to unoccupied *nearest* neighbour sites in one time step $t \rightarrow t + \Delta t$, i.e. $v_{\mathrm{max}} = 1$ cell/time step. This constraint corresponds to a maximum empirical walking speed of $v_{\mathrm{emp}} = 1.3$ m s^{-1} [14, 15], if the timescale Δt is identified with 0.3 s. The choice $v_{\mathrm{max}} = 1$ has the advantage of simplicity and high simulation speed. It also reproduces most experimentally observable phenomena. Nevertheless, there are reasons for the introduction of higher walking speeds $v_{\mathrm{max}} > 1$ in some cases:

(i) Figure 1 shows the fundamental diagram of the flow along a corridor in the $v_{\mathrm{max}} = 1$ case of large coupling k_S and $k_D = 0$.[7] It is nearly symmetric with maximal flow at

[7] The empirical unit of the specific flow is pedestrians m^{-1} s^{-1}, the natural unit of the model: particles/$(a\Delta t)$ (with cell length $a = 40$ cm and timescale Δt).
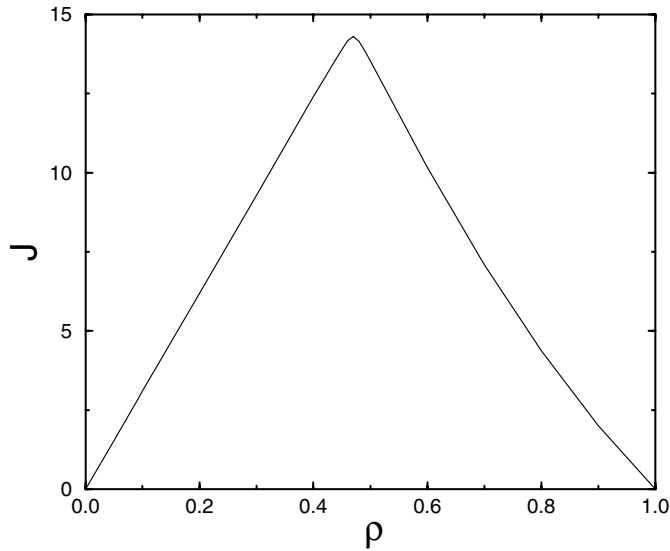
Figure 1. The fundamental diagram (flow J, measured in units of $1/\Delta t$, versus density ρ, measured in units of $\rho_{\max} = 1/a^2 = 6.25 \text{ m}^{-2}$) for a corridor of 93×33 lattice cells of size $a^2 = 40 \times 40 \text{ cm}^2$ with $v_{\max} = 1$ in the so-called ordered regime ($k_S = 10.0$ and $k_D = 0.0$). The static floor field S is calculated using a Manhattan metric. In the direction of the flow, periodic boundary conditions are used. For details see [7, 24].

$\rho \approx \frac{1}{2}$. However, experimental data point to a non-symmetric fundamental diagram with maximal values of the flow for densities $\rho < \frac{1}{2}$ [14, 15].

(ii) The interaction horizon is not isotropic since pedestrians react mainly to stimuli in front of them. This anisotropy can be better taken into account in a model with larger interaction range where it is generated dynamically through the exclusion principle.

(iii) Although the velocity distribution of a pedestrian is sharply peaked around 1.3 m s^{-1}, higher walking speeds are frequently observed [14, 15].

(iv) In a model with $v_{\max} > 1$, a realistic distribution of different walking speeds of the particle ensemble can be implemented in a simple way.

Certainly the most relevant aspects are the first two. The other two requirements could be taken into account in the case $v_{\max} = 1$ by introducing individual randomization probabilities, determined by the coupling constants k_S and k_D, or a rescaling of the relevant timescale. In the following, extensions of the model to $v_{\max} > 1$ will be presented. The possible variants of the update algorithm and their dynamical properties will be discussed in detail and compared to experimental data.

3.1. Classification of the model variants

In the case of $v_{\max} = 1$, the particles are allowed to cover a maximal distance of $a = 40 \text{ cm}$ (corresponding to a movement to next neighbouring sites) per time step. Then for higher walking speeds $v_{\max} \geq 2$ the particles should be able to cover a distance of $v_{\max}a$ in one time step. This does not necessarily correspond to higher velocities, e.g. when
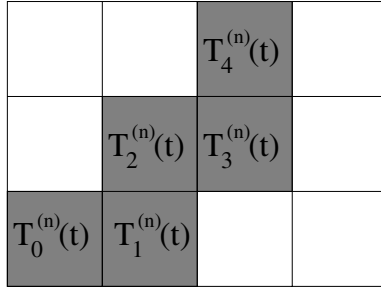
Figure 2. A graphical representation of the desired trajectory $T_l^{(n)}(t)$ of pedestrian n for the case $v_{\max} \geq 4$.

combined with a reduction of the cell size or change of timescale, which is the case mainly considered here. Then, due to the two-dimensional nature of the motion, the chosen path is not necessarily straight. Also, it has to be taken into account that now the paths of different pedestrians may cross. This requires a generalization of the concept of friction. In the following we develop a formalism which allows us to describe the different possible generalizations.

At the beginning of a time step t the position of each particle $n \in \{1, \ldots, N\}$ is denoted by $T_0^{(n)}(t)$. Each particle then chooses, corresponding to its desired movement, a trajectory $T^{(n)}(t) = \{T_0^{(n)}(t), \ldots, T_{v_{\max}}^{(n)}(t)\}$ consisting of $v_{\max} + 1$ lattice sites. The single elements of $T^{(n)}(t)$ are determined by applying the update rules $\mathcal{Z}$ for the $v_{\max} = 1$ case successively $v_{\max}$ times. Here, every arbitrary element $T_l^{(n)}(t)$ $(l > 0)$ corresponds to a target site $\mathcal{Z}$ of the particle n that has advanced virtually to site $T_{l-1}^{(n)}(t)$ (see figure 2):

$$T_l^{(n)}(t) = \mathcal{Z}(T_{l-1}^{(n)}(t)). \tag{1}$$

Therefore, $T_l^{(n)}(t)$ can only be one of the four next neighbour sites of $T_{l-1}^{(n)}(t)$ or $T_l^{(n)}(t) = T_{l-1}^{(n)}(t)$. Thus, every particle accesses iteratively at most $v_{\max}$ target sites. It is important to notice that the $v_{\max}$ target sites and thus the trajectories are determined using the configuration of the system at time t through $\{T_0^{(1)}(t), \ldots, T_0^{(N)}(t)\}$.

All desired trajectories can be summarized in the matrix

$$T(t) = \begin{pmatrix} T_0^{(1)}(t) & \cdots & T_{v_{\max}}^{(1)}(t) \\ \vdots & \ddots & \vdots \\ T_0^{(N)}(t) & \cdots & T_{v_{\max}}^{(N)}(t) \end{pmatrix}, \tag{2}$$

which has to be stored at every time step of the simulation. Two basic assumptions of the model are reflected by the matrix elements of $T(t)$:

- Hard core exclusion of particles: $T_0^{(i)}(t) \neq T_0^{(j)}(t)$ for all $i \neq j$; i.e. every lattice site can be occupied by at most one particle.

- Parallel updating: $T_{v_{\max}}^{(i)}(t) \neq T_0^{(j)}(t)$ for all $i \neq j$. This expresses the reaction time of the particles. No particle can occupy a lattice site at time step $t + 1$ which was occupied at time step t by another one.

These properties are special cases of the more general rule $T_n^{(i)}(t) \neq T_0^{(j)}(t)$ for all $i \neq j$ and $n = 0, 1, \ldots, v_{\max}$. They restrict the allowed values of the first and last column of $T(t)$, i.e. the allowed positions at time t and $t + \Delta t$. The remaining $v_{\max} - 1$ columns correspond to intermediate states that are not explicitly realized as configurations. It might happen that two or more desired trajectories cross or that even one of the intermediate states violates the hard core exclusion principle. In the following we will denote such situations as *conflicts*. In principle, one could ignore the existence of conflicts since they correspond only to virtual intermediate states. However, in order to make the dynamics more realistic it is necessary to take them seriously. Then a method for the resolution of conflicts is required. In the following we will discuss four major variants.

3.1.1. Hop or stop. The simplest variant ignores the intermediate positions $T_l^{(n)}(t)$ $(l = 1, \ldots, v_{\max} - 1)$ and takes only conflicts in the desired new positions $T_{v_{\max}}^{(n)}(t)$ into account. If k particles $(k \geq 2)$ have chosen the same target cell, i.e.

$$T_{v_{\max}}^{(i)}(t) = T_{v_{\max}}^{(j)}(t), \qquad \text{for all } i, j \in \{1, \ldots, k\}, \tag{3}$$

one particle i is chosen by a probabilistic method (i.e. in random order) and is allowed to move to target site $T_{v_{\max}}^{(i)}(t) =: T_0^{(i)}(t + 1)$. The other $k - 1$ particles $j \neq i$ involved in the conflict are not allowed to move and have to remain at their origin sites, i.e. $T_0^{(j)}(t + 1) = T_0^{(j)}(t)$. Practically, this can be easily implemented by allowing all particles to move sequentially by choosing randomly a permutation σ of the particle indices j that determines the order $\sigma(j)$ of updating[8].

This is the simplest form of conflict resolution between particles. The overall movement takes place without consideration of the trajectories $T^{(n)}(t)$. Crossing trajectories and jumping over already advanced particles are permitted in order to keep the spirit of the parallel updating scheme.

3.1.2. Move as far as possible. This variant of conflict resolution is similar to the previous one. Again the particles are allowed to move in random order described by a randomly chosen permutation σ. However, now other particles that have already reached their target sites cannot be jumped over by following particles any longer. A particle n is able to proceed along its trajectory $T^{(n)}(t)$ as long as $T_l^{(n)}(t)$ $(l \in \{1, \ldots, v_{\max}\})$ is not already occupied by another particle.

In this variant, crossing trajectories are still possible, but jumps over particles that have already reached their target sites are not allowed.

3.1.3. $v_{\max}$ sub-steps. In this variant of the update the particle movement along the trajectories $T_n(t)$ is subdivided into $v_{\max}$ sub-time steps where moves to nearest neighbour cells are allowed. If in one sub-time step l, two or more (at most four) particles try to move to the same cell, i.e.

$$T_l^{(i)} = T_l^{(j)}, \qquad \text{for any } i, j, \tag{4}$$

---

[8] This implies that the particles move in the order $\sigma^{-1}(1), \sigma^{-1}(2), \ldots, \sigma^{-1}(N)$.

only one randomly chosen particle is allowed to move forward to this site. All other particles then try to reach the site during the next sub-time step $l + 1$.

In all sub-time steps of this update version conflicts between particles are taken into account and solved. Therefore, it is the easiest way to incorporate the concept of friction [8] into the model with $v_{max} > 1$. Otherwise, this method leads to increased simulation times due to the successive treatment of the sub-time steps. Note that the dynamics of this variant is different from the genuine $v_{max} = 1$ case, since the trajectories $T^{(n)}$ are fixed during the whole time step.

3.1.4. No crossing paths. In this last version, no particle is allowed to cross the trajectory of a particle that has already moved. The particles move in random order. If the path of particle n crosses that of a particle n' that has already moved (i.e. $\sigma(n') < \sigma(n)$),

$$T_l^{(n)} = T_k^{(n')}, \qquad \text{with } l, k \text{ arbitrary,} \tag{5}$$

then

$$T_0^{(n)}(t + 1) = T_{l-1}^{(n)}(t). \tag{6}$$

k is in this case assumed to be the smallest index in the trajectory of n' for which this condition holds. Therefore, in this variant a particle is allowed to move until it reaches a cell that is either occupied or has been passed by a previous particle that has already been moved at the same time step.

3.1.5. General aspects of the variants. In all variants, at the end of each time step the field values of the dynamic field D at all lattice sites of the trajectories traversed by particles are increased by one. Afterwards D is modified by its decay and diffusion dynamics as described in [6, 7].

Each of the four update versions is stressing different aspects of the two-dimensional motion on the lattice. Figure 3 shows a representation of all different methods for conflict resolution. All four variants reduce to the basic model described in section 2 in the case of $v_{max} = 1$.

The characteristic timescale Δt should not be influenced by the choice $v_{max} > 1$. Therefore, for a given value of v_{max} the corresponding maximum empirical walking speed can be calculated via

$$v_{max}^{(emp)} = v_{max} \frac{a}{\Delta t} = v_{max} \times 1.3 \text{ m s}^{-1} \tag{7}$$

with $a = 40$ cm and $\Delta t = 0.3$ s.

In the following, the consequences of higher walking speeds for particle flows will be investigated and the differences between the four variants discussed. Afterwards, the dependence of the evacuation time for a room on v_{max} is investigated.

3.2. Simulations

The particle flows $J = \rho \langle v_x \rangle$ presented in this section are measured in a corridor of size $X \times Y = 93 \times 33$ with periodic boundary conditions in the x-direction. The motion in the y-direction is limited by walls. The static floor field S increases from left to right, i.e. $S_{x,y} = x$ [16]. We remind the reader that in the floor field model a motion
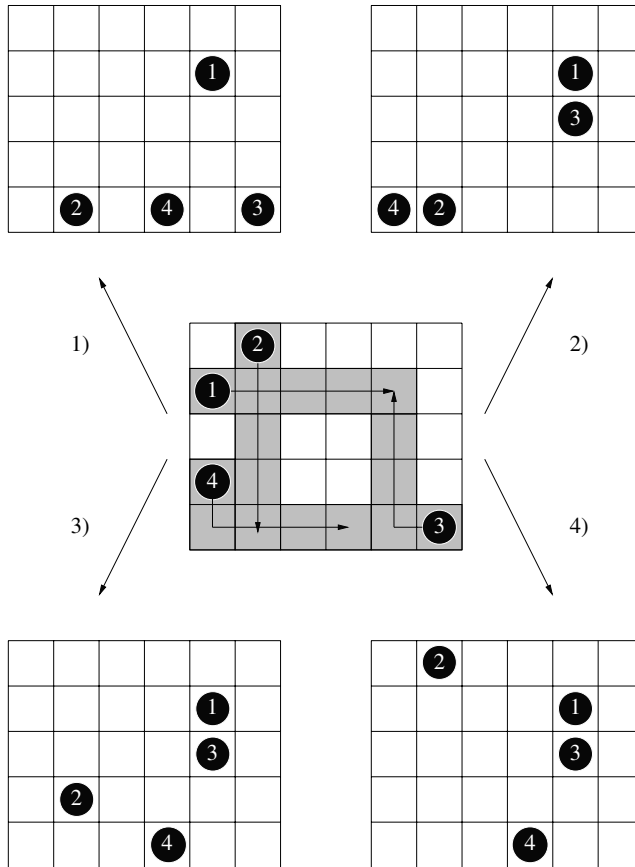
Figure 3. A graphical representation of all variants of conflict resolution in the case $v_{\max} = 4$. The trajectories $T^{(n)}(t)$ of the particles are shaded grey. The numbers of the particles correspond to the random order (given by the permutation σ) in which the particles execute their steps. In variants (1), (2) and (4) this order is designated once. In the variant (3) one has to choose a new random order in every single sub-time step.

in the direction of increasing field strength is preferred. The lattice was initialized by randomly distributing N pedestrians corresponding to a density $\rho = N/(XY)$. If not stated otherwise, the coupling k_D to the dynamical field vanishes ($k_D = 0$) and therefore the dynamical parameters of D can be chosen as $\alpha = 0$ and $\delta = 1$.

3.2.1. Fundamental diagrams for different values of $v_{\max}$. Figure 4 shows fundamental diagrams for $v_{\max} = 1, \ldots, 5$ for two of the variants discussed above. In figure 4(a) the flow values J are shown for the case of a dominating coupling to the static field ($k_S \gg k_D$, corresponding to the ordered regime [7]). The update is based on the *no crossing paths* variant. The maximal flow is reached at smaller particle densities for growing $v_{\max}$. The maximal flow is also increasing with $v_{\max}$. An unexpected property of this variant is that for densities $\rho > 0.4$ the flow J is largest in the case $v_{\max} = 1$. This can be explained by the blockage of wide parts of the lattice, resulting from the non-traversable trajectories of the particles. The influence of this blockage increases with $v_{\max}$ due to an increased
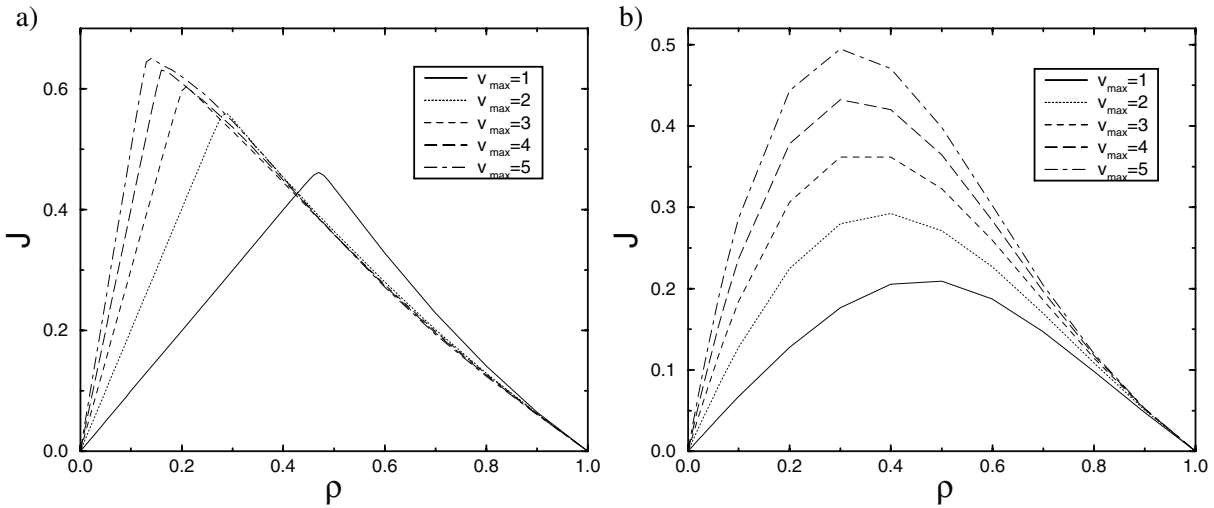
Figure 4. Fundamental diagrams for $v_{\max} = 1, \ldots, 5$. (a) Variant 4 (*no crossing paths*) with $k_S = 10.0$ and $k_D = 0.0$; (b) variant 2 (*move as far as possible*) with $k_S = 2.0$ and $k_D = 0.0$.

'effective density'. The faster a pedestrian moves, the more cells she or he blocks. In this respect, the *no crossing paths* scheme leads to the highest effective densities (figure 4).

Because of the strong coupling to the static field S, which suppresses swaying in the y-direction, the fundamental diagrams look very similar to those of the ASEP or other traffic models in the deterministic limit (figure 4(a)). If one chooses, like in figure 4(b) for the second version of the update, a smaller coupling strength ($k_S = 2$), the effective walking speed v_{eff} of the particles is decreasing. For $k_S \to \infty$ the effective walking speed of a single pedestrian is $v_{\text{eff}} \to v_{\max}$, corresponding to a deterministic motion. On the other hand, for $k_S = 0$ the particle performs an isotropic random walk since the information about the preferred direction through the static floor field is not taken into account. Therefore, for $k_S = 2.0$ the shape of the fundamental diagrams is becoming smoother (figure 4(b)). The maximal values of J are smaller with a slight shift of the maximum to higher densities (for $v_{\max} > 1$) and the slopes in the regions of small and high densities decrease.

In the following, the consequences of the different conflict resolution schemes for the flow are discussed. Figure 5 shows the fundamental diagrams of all four variants for the velocities $v_{\max} = 2$ and 4 and $k_S = 2.0$. For $v_{\max} = 2$ the differences between the variants are not strongly pronounced (figure 5(a)). But the flow values J are highest for the $v_{\max}$ *sub-steps* and smallest for the *no crossing paths* scheme in all density regions.

However, for $v_{\max} = 4$ the differences between the variants are easy to spot. For particle densities $\rho > 0.1$ the *no crossing paths* scheme produces much smaller flow values than all other variants, because of the non-traversable trajectories which are four sites long. The third version of the update (*sub-steps*) leads to the highest flows in all density regions since the resolution of conflicts in sub-time steps enables some particles to move forward in a later sub-time step.

Finally, we compare the simulation results with empirical data. Figure 6 shows a comparison of fundamental diagrams of the variant with $v_{\max}$ *sub-steps* (see section 3.1.3) with a fit of empirical flow–density relations [14]. The data for the specific flow have been
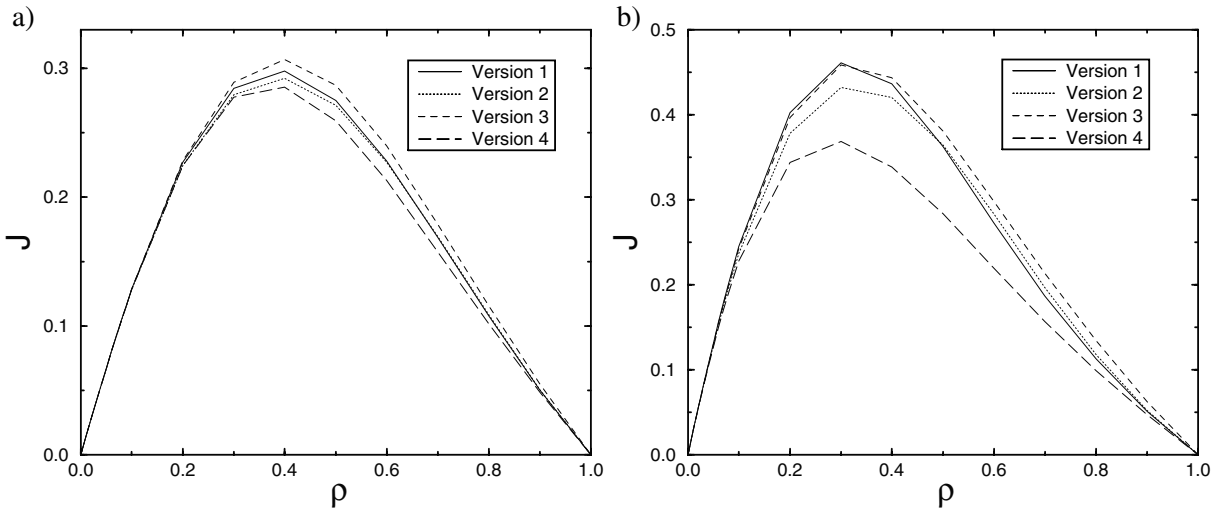
Figure 5. Fundamental diagrams for all four update variants with $k_S = 2.0$ and $k_D = 0.0$: (a) $v_{\max} = 2$; (b) $v_{\max} = 4$.

transformed into the units of the model. The fundamental diagram for $v_{\max} = 3$ is in good agreement with the experimental data. In particular, the density values for the highest flow match each other very well. Since $k_S = 4.0$, the particles have a reduced effective walking speed $v_{\mathrm{eff}} < v_{\max}$. In the model, this results in a diversification of the flows for particle velocities between $v_{\max} = 3$ and lower values. For high density regions $\rho > 0.6$ the model yields flow values which are too small. The reason is lane changes of particles especially at higher densities. If the site infront of a particle is occupied, lane changes are possible. Such a changing does not increase the flow in the positive x-direction, but often inhibits the movement of another particle (see figure 7). The fundamental diagrams of the other $v_{\max}$ values do not agree as well with the empirical data.

3.3. Simulation of the evacuation of a room

As a second scenario which helps to understand the effects of $v_{\max} > 1$ we investigate its influence on evacuation times. The room to be evacuated is a square of 63×63 cells. The exit has a width of one cell and is located at the centre of one wall. Initially the particles are distributed randomly and then try to leave the room due to the information that they get through the floor fields. This scenario has been studied in detail in [7] where three different regimes (*ordered* for $k_S \gg k_D$, *disordered* for $k_D \gg k_S$ and *cooperative*) have been identified.

Figure 8 shows averaged evacuation times for different combinations of the coupling parameters k_S and k_D for the *move as far as possible* variant of the update. All other schemes show the same qualitative behaviour. The particle velocities are $v_{\max} = 1, \ldots, 4$. Figure 8(a) can be interpreted in the following way: if the coupling strength to the static field S is very small ($k_S \ll 1$), the particle motion resembles a random walk. But even if there is only slightly directed movement, the variance in lateral direction is increased with $v_{\max}$. Therefore, the particles can reach the exit by chance faster for increased $v_{\max}$, resulting in decreased evacuation times. In the limit $k_S \to \infty$ the particles move on the
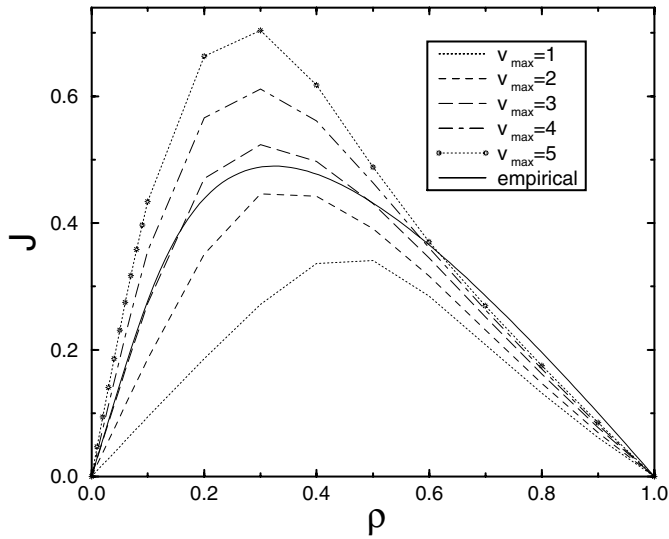
Figure 6. Comparison of fundamental diagrams of the third update version and the velocities $v_{\max} = 1\text{--}5$ with experimental data from [14] ($k_S = 4.0$ and $k_D = 0.0$).
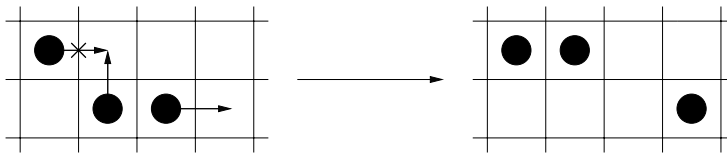

Figure 7. The decrease of the flow due to lane changes.

shortest possible way to the exit; the movement becomes deterministic. For higher particle densities just after the evacuation starts a big jam forms in front of the exit. Therefore, the averaged evacuation times are in this case determined by the particle number (via the flow through the door) rather than the maximum walking speed. Thus, for higher densities and $k_S \to \infty$ the evacuation times using the *move as far as possible* strategy (see figure 8 top) are the same for all $v_{\max}$ values.

A coupling strength of $k_S \gg 1$ is presumably the most relevant for a comparison with real pedestrian behaviour. Therefore, for many applications the restriction to $v_{\max} = 1$ is adequate to reproduce realistic behaviour. In other cases (see above) a choice of $v_{\max} > 1$ is indispensable.

Finally, figure 8(b) shows the different evacuation times for $k_D = 0.0$ and varying $v_{\max}$. Since k_S is very small ($k_S = 0.4$), they are decreasing with $v_{\max}$. The characteristic non-monotonic behaviour for increasing k_D (see [7]) is reproduced for all $v_{\max}$ values. Since in this parameter regime the particle density is a restricting factor for the evacuation time due to the clogging occurring at the exit, for $v_{\max} \geq 2$ one finds some kind of convergence of the time values.
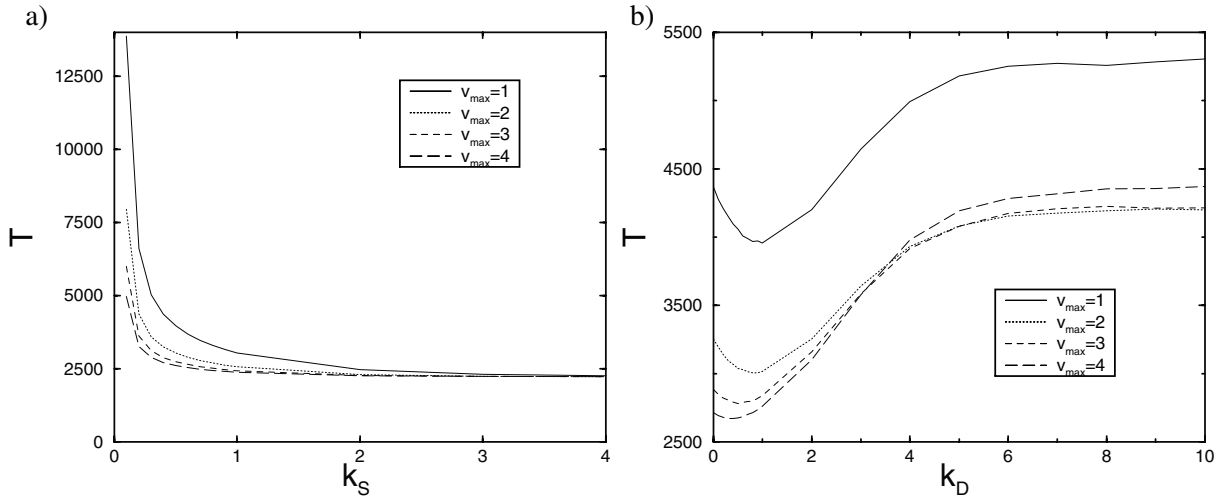
Figure 8. Averaged evacuation times for a room of size 63×63 sites and an exit of one cell. The particle density at the beginning of the evacuation is $\rho = 0.3$ (1116 randomly distributed particles). Different $v_{\max}$ values in the second version of the update (*move as far as possible*). (a) $k_D = 0.0$; (b) $k_S = 0.4$; and $\delta = 0.3$ and $\alpha = 0.0$ as parameters for the dynamics of D.

4. Finer discretization of space

Increasing the maximal velocity of pedestrians is not the only modification that influences the realism of the model. One of the boldest assumptions in CA models for pedestrian motion is the representation of space as a grid of cells and the corresponding restriction of the spatial resolution to the cell size, in this case 40 cm. However, it can be argued that this simplification is justified by the reaction time (or decision time) which can be easily identified in the model. Nevertheless, a—preferably qualitative—investigation of the discretization effects would shed some light on the issue. The space discretization used so far has been chosen in the simplest possible way such that a pedestrian occupies only one cell. This leads to a length scale of $a = 40$ cm (see section 2). However, for some applications this might not be adequate and a finer discretization is necessary. In the following we will discuss the necessity of a smaller length scale, ways of implementing it and the consequences for the behaviour of the model.

4.1. Motivation and consequences

The identification of the size of one lattice site with the typical space occupied by a pedestrian in a dense crowd is most natural for the construction of a CA model for pedestrian dynamics. For square cells this leads to a cell size of $a^2 = 1/\rho_{\max}^{(\mathrm{emp})}$ and $a = 40$ cm where $\rho_{\max}^{(\mathrm{emp})} \approx 6.25$ persons m^{-2} is the maximal empirically observed density [14]. All units of space are then multiples of the length scale $a = 40$ cm. In contrast to the introduction of higher velocities discussed in the previous section which was motivated by the unrealistic shape of the fundamental diagram, there are no simulation results that indicate the necessity of a better spatial resolution. Nevertheless, there are good reasons
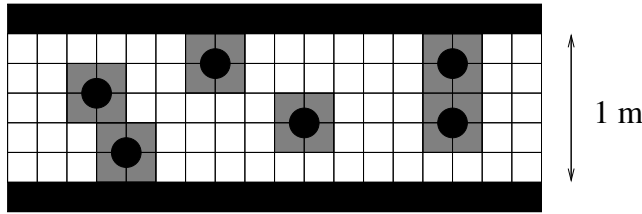
Figure 9. Representation of a corridor of width 1 m in the 20 cm model. Such a corridor cannot be reproduced exactly in the 40 cm model. The four cells occupied by each particle are shaded grey.

to introduce a finer discretization of space.

(i) If the model is used not only for basic investigations of pedestrian dynamics, but also for the assessment of evacuation scenarios in complex structures (such as passenger vessels and football stadiums), an accurate representation of the geometries is desirable. A finer discretization corresponds to a more accurate representation of geometrical structures in a natural way. This can be seen from figure 9.

(ii) As we have seen in section 3, some situations require the use of higher velocities $v_{\max} > 1$. If one wants to keep the timescale unchanged this has to be compensated by introducing a smaller length scale.

(iii) In principle, it would be interesting to consider the continuum limit $a \to 0$ in order to make contact with models that are based on a continuous representation of space, e.g. the social force [26, 29] and similar models [30] or hydrodynamic approaches [31]–[35].

The straightforward approach for investigating the discretization effects is to vary the cell size. If one chooses a cell size of $a = 20$ cm, the area $A = 1/\rho_{\max}^{(\mathrm{emp})}$ occupied by a pedestrian is four cells (see figure 9), in order to reproduce the maximal density $\rho_{\max}^{(\mathrm{emp})}$. The natural generalization for the allowed motion of the original model as described in section 2 (in the following denoted as the 40 cm model) is the motion of the centre of a pedestrian by one cell (i.e. a distance a; see figure 10). This is only possible if the two neighbouring cells are unoccupied. As can be seen from the relation (7) (with $v_{\max} = 1$) for the three fundamental quantities the time step Δt in the 20 cm model is half as long as in the 40 cm model[9]. For the empirical velocity of $v_{\mathrm{emp}} = 1.3$ m s^{-1} and $a = 20$ cm the timescale is $\Delta t = 0.15$ s. For an arbitrary spatial discretization a one obtains the timescale $\Delta t = a/v_{\max}^{(\mathrm{emp})}$.

Finer discretizations of the underlying geometric structure for fixed velocity $v_{\max}$ therefore lead to smaller scales of length and time of the model. So the limit $a \to 0$ results in a space *and* time continuous model. This limit allows a comparison between discrete and continuous models, but is not considered here.

The occupation of four lattice sites by one particle has further consequences in the 20 cm model, especially for the floor field model described in section 2.

---

[9] An extension of the 20 cm model to a model with walking speeds $v_{\max} > 1$ is possible in the same way as discussed in the previous section, but will not be considered in the following.
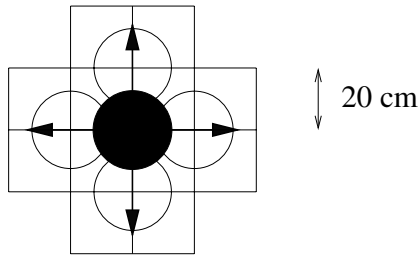
Figure 10. Occupation of 2×2 lattice sites of cell length $a = 20$ cm and possible transitions in a time step.
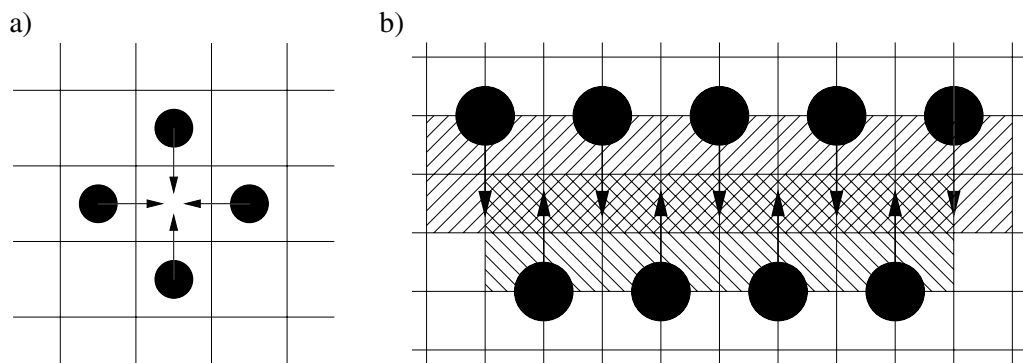

Figure 11. (a) Typical local conflict in the 40 cm model. (b) In the 20 cm model in principle all particles of a system can be part of a conflict. Hatched cells contribute to the non-local conflict.

 (i) Every particle leaves two of the four cells that it occupied previously (figure 10). In both these cells the dynamic floor field has to be increased.

(ii) Since a particle always occupies four lattice sites, the transition probabilities are calculated by averaging the specific field values of static and dynamic floor fields S and D.

In any CA, not only the floor field model, an important new effect related to conflicts occurs when the cell size is reduced and particles occupy more than just one cell. In the 40 cm model, conflicts can be described as *local* interactions (figure 11(a)), because only a small number of particles can access the same lattice site which is determined by the coordination number of the lattice. On the other hand, in the 20 cm model conflicts are not necessarily local any longer. Here, conflicts are not restricted to single cells and can spread over a wider area of the lattice. This is illustrated for a typical situation in figure 11(b). Assume that the permutation σ (see section 3.1.1) is such that the particles move from 'left to right', i.e. all the particles in the top row are allowed to move and the particles in the bottom row are not. Switching $\sigma^{-1}(1)$ and $\sigma^{-1}(2)$ will change the movement of all particles. This is not the case for particles that occupy only one cell, i.e. $a = 40$ cm.

In the floor field model conflicts allow for the introduction of friction parameter μ [8, 16] (see section 2). Due to the possible non-local nature of conflicts in the 20 cm model
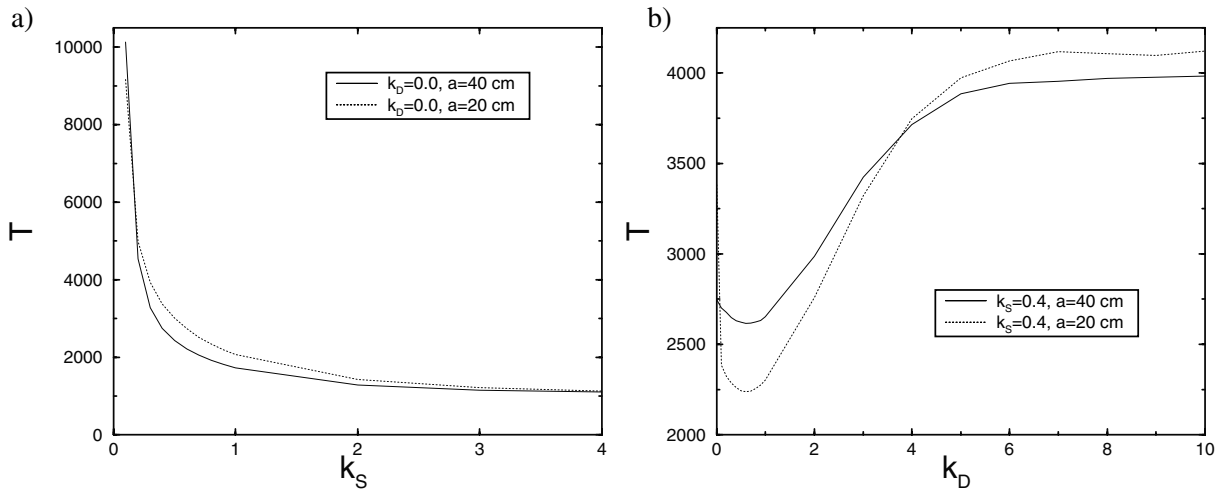
Figure 12. Averaged evacuation times for a room of size $62 \cdot 40$ cm $\times$ $62 \cdot 40$ cm and an exit of width 80 cm: (a) $k_D = 0.0$ fixed and variation of k_S; (b) $k_S = 0.4$ fixed and variation of k_D ($\delta = 0.3$ and $\alpha = 0.0$).

this concept cannot be straightforwardly generalized. New concepts for the description of conflicts are necessary, which is currently under investigation and will be discussed in a future publication.

In the next section, simulation results for the 20 cm model will be compared to results for the conventional model.

4.2. Simulation results

4.2.1. Evacuation times. First, we will turn to the influence of the discretization on evacuation times. We measured the averaged times of the evacuation of a large single room with an area of about $(24.8 \text{ m})^2$, corresponding to 62×62 cells for the $a = 40$ cm model or 124×124 cells for the $a = 20$ cm model. The particles leave the room via a door of width 80 cm (two or four lattice sites, respectively). Figure 12 shows the impact of the variation of the parameters k_S and k_D in the $a = 20$ and 40 cm models[10]. The initial particle density is $\rho = 0.3$ corresponding to 1153 particles. The qualitative behaviour of the model when varying the parameters (see section 3 and [7]) is not influenced by the finer discretization. Because of slightly different transition probabilities due to the averaging of the field values of four sites for each walking direction in the $a = 20$ cm model, small deviations only exist for coupling strengths $k_S < 3$ (see figure 12(a)). This also leads to different time values for the parameter choice $k_D = 0.0$ and $k_S = 0.4$ in figure 12(b). It is remarkable that the effect of the non-monotonic parameter dependence [7] of the curve is most pronounced in the $a = 20$ cm model.

The most important difference between the 20 cm and 40 cm models is the possibility of a deadlock in front of a small exit. Consider the flow through a bottleneck of the dimension of the particle width (i.e. the bottleneck and particle have the width of two

---

[10] The times are measured in update steps. Therefore, for a comparison of the two models, the simulation times of the $a = 20$ cm model have to be divided by two.
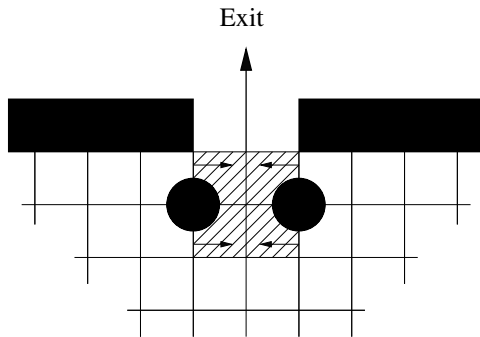
Figure 13. Blockage of bottlenecks or exits of width 40 cm in the 20 cm model caused by two particles. Both particles try to access the four lattice sites in front of the exit.

cells or 40 cm). If two particles reach the bottleneck at the same time step, their mutual blockage (see figure 13) may lead to vanishing flows. Similar observations have been reported in experimental investigations (see e.g. [36, 37]). This phenomenon can occur in pushing pedestrian crowds at bottleneck-shaped exits of small width. It has also been observed for some continuum pedestrian models with extended particles [27] and similarly in granular flow through a funnel [38, 39]. Therefore it is remarkable that it does *not* appear in the original 40 cm model.

On the other hand, the movement itself is more effective for the 20 cm model compared to the 40 cm model. For very high values of k_S, the overall evacuation time is determined by the outflow through the door. In the case considered here ($w = 80$ cm $= 4$ cells if $a = 20$ cm), the blockage basically does not occur. For very low values of k_S (cf figure 12), the particles perform a random walk and therefore the discretization ($a = 20$ cm versus $a = 40$ cm) does not play a prominent role. This interpretation is also supported by the results shown in figure 15 where the smallest possible exit is investigated. In this case, the flow increases with the density for small coupling strengths k_S and increases with large coupling strengths. However, this does not really explain the subtle differences in the area $0.5 \leq k_S \leq 2$, which will be investigated in more detail at a later point.

4.2.2. Flow measurements. The discretization has a significant influence on the flow. Figure 14 shows the fundamental diagrams in the ordered regime for a corridor of width 2 m (i.e. width five lattice sites in the $a = 40$ cm model and ten lattice sites in the $a = 20$ cm model). The flows of both models are identical up to $\rho \approx \frac{1}{2}$. The density region $\rho < \frac{1}{2}$ characterizes in both models the free flow regime. Nearly all particles can move to their right next neighbour site in each time step; the flow increases linearly with the density. For a density of $\rho \approx \frac{1}{2}$, the probability of occupied next neighbour sites is greatly increasing in the 40 cm model, so the average velocity of the particles is decreasing to a value $\langle v_x \rangle < 1$. Therefore, the flow decreases with increasing density and is additionally decreased by lane changing events (see figure 7).

The behaviour is different in the 20 cm model: the space that a particle needs for unimpeded movement in one time step corresponds to only half the length of its own size. Therefore, the average particle velocity is $\langle v_x \rangle \approx 1$ up to a density of $\rho \approx \frac{2}{3}$, which leads
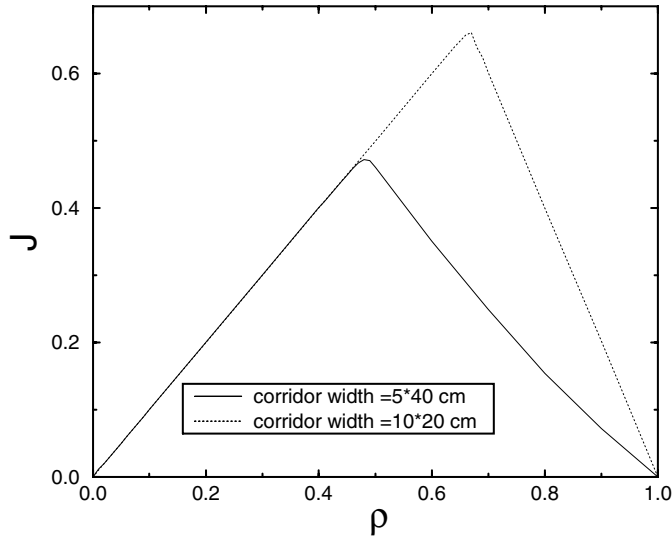
Figure 14. Fundamental diagrams in the ordered regime ($k_S = 10.0$, $k_D = 0.0$) for both model variants. Width of corridor: five cells in the 40 cm model and ten cells in the 20 cm model.

to a linear increase of the flow up to this density. For $\rho > \frac{2}{3}$ one finds a sharp decrease of the flow.

Thus the finer discretization results in a shift of the maximum flow to regions of higher density. This effect will be present for even finer discretizations. As in section 3, experimental data point to a realistic flow maximum for densities $\rho < \frac{1}{2}$. Therefore the 20 cm model (with $v_{max} = 1$) cannot reproduce these results qualitatively.

Figure 15 shows the flow J through a bottleneck of width 40 cm versus the parameters k_S and ρ. Only for very small k_S ($k_S = 0.1$) is a small particle flow sustained for higher densities. For increasing k_S the flow breaks down at very small densities (for $k_S = 10.0$ the flow is zero for all densities). The system freezes for growing strength of coupling, k_S, to the static floor field. This is somewhat similar to the paradoxical *faster-is-slower effect* [2, 27], as an increasing k_S implies higher individual walking speeds. The clogging effect observed in our model is due to the local blockage shown in figure 13.

5. Conclusion

We have systematically investigated the influence of the interaction range v_{max} and the spatial discretization a on the behaviour of two-dimensional CA models for pedestrian motion. Using simulations of a corridor and evacuation from a large room we have shown that both parameters can have a significant influence on the properties of the model. Although we have used a specific model, the floor field CA, for our simulations due to its ability to reproduce the observed *collective* phenomena correctly, we believe that the effects discussed here are generic for any discrete approach to pedestrian dynamics. Of course this requires further investigation in the future.

First we considered the extension of the interaction range which we have implemented through a larger walking speed v_{max}. We have seen that there are different possibilities for
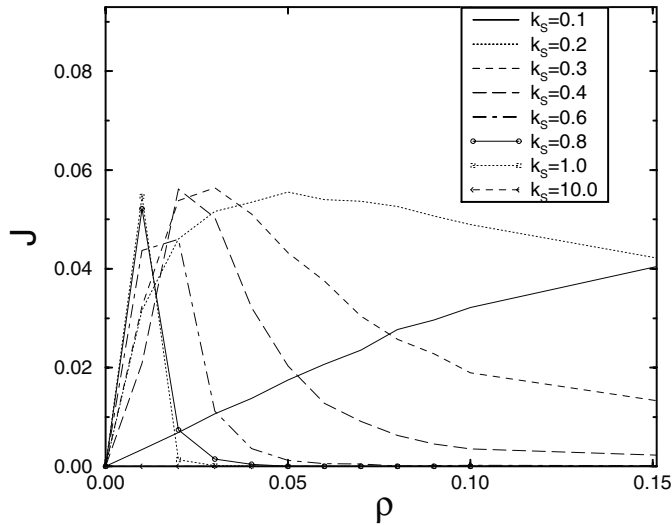
Figure 15. The fundamental diagram of a corridor (93×33 cells of size 40 cm $\times$ 40 cm) with a bottleneck of width 40 cm. The couplings to the static and dynamic floor fields are k_S and $k_D = 0.0$.

achieving this. This modification leads to a considerable improvement of the agreement of fundamental diagrams for the motion along a corridor with empirical findings. In the original case $v_{\max} = 1$, the fundamental diagram of the model was almost symmetric with respect to the density $\rho = 0.5$. The reason is that for a such a unidirectional motion where swaying is strongly suppressed many models effectively reduce to a number of independent ASEPs[11] and hence the observed flow–density relation reflects its particle–hole symmetry. As in models of highway traffic [17] the maximum in the homogeneous case is shifted to lower densities for larger $v_{\max} = 2$ and thus leads to a more realistic approach.

As a second scenario we have studied the evacuation from a large room. Here it turned out that in most cases the results are not affected strongly by the introduction of a larger velocity $v_{\max}$.

Summarizing, these results indicate that the choice $v_{\max} = 1$ might not in all cases be justified. As indicated above, the fact that for the corridor one has to deal with a basically one-dimensional motion is important. Here it is remarkable that for a continuum model such as the social force model this problem also requires a rather different choice of interaction parameters [37] compared e.g. to evacuation problems, especially as regards the repulsive interaction forces. This shows that both model classes have to be generalized in order to achieve a proper description of all possible situations in a unified way.

The case of the second non-trivial fundamental parameter, namely the cell size, is even more intricate. A finer spatial discretization does not only provide a connection to a different class of microscopic models based on continuous representation of space. In many applications to real life problems the geometries under consideration cannot be described by lengths that are multiples of the length scale $a = 40$ cm of the original model. We have argued that a reduction of this length scale, and thus the cell size, must be accompanied

---

[11] One could expect that in the case of a mixture of species with different $v_{\max}$ the decoupling of the lanes will be less pronounced.

by an increase of the size of the particles. In order to reproduce the empirically observed maximal density they have to now occupy more than one cell, e.g. four in the case of $a = 20$ cm. If the particles have the same symmetry as the underlying lattice this also restricts the allowed length scales. For example, for the square lattice the most natural extensions of the particles are $2^n \times 2^n$ cells corresponding to a length scale $a_n = 40/n$ cm.

By studying the same two scenarios as for the influence of $v_{\max}$ we found two main consequences of using a finer discretization. On the one hand, the flow is increased since the particles can now move ahead if there is space available that is less than their own size. On the other hand, particles can now block each other more easily. This might lead to non-local conflicts where groups of pedestrians mutually block each others motion (figure 11). Furthermore, at exits, blocking can result in a complete breakdown of the outflow. This is not related to the discreteness of the model and can also be observed in continuum models with particles of finite size.

It would be interesting to take the continuum limit of our model to relate it to other continuum approaches. A naive continuum version of the floor field model is currently under investigation and might serve as a reference model. Our present study has shown that finer discretization or larger velocities in combination with a discrete time (parallel) dynamics leads to the possibility of complicated conflict situations. One could try to solve this problem by using a continuous time dynamics, but this might drastically increase the computational complexity of the model in a different way.

Even though our investigations are based on a square grid (one could also think of a hexagonal lattice, and indeed there are models based on this [40, 41]) the results obtained are generally valid. As a next step, currently the combined effect of larger $v_{\max}$ and smaller cells is being investigated. Then one can expect to encounter a combination of many effects observed here. However, e.g. in the case of flow along a corridor, these modifications have opposite quantitative effects. Whereas an increase of $v_{\max}$ tends to shift the location of maximal flow to smaller densities the reduction of the length scale has the opposite effect. This work is in progress and will be reported elsewhere.

Summarizing, we can say that discrete models such as cellular automata yield quite realistic results. For example, the floor field model is able to reproduce collective effects (such as lane formation in counterflow) observed empirically. However, for applications where a reliable *quantitative* prediction should also be made, one has to take some care in the choice of the basic parameters such as cell size and interaction range.

References

[1] Schreckenberg M and Sharma S D (ed), 2001 *Pedestrian and Evacuation Dynamics* (Berlin: Springer)
[2] Helbing D, 2001 *Rev. Mod. Phys.* **73** 1067
[3] Nagatani T, 2002 *Rep. Prog. Phys.* **65** 1331
[4] Rothman D H and Zaleski S, 1997 *Lattice-Gas Cellular Automata* (Cambridge: Cambridge University Press)
[5] Gershenfeld N, 1999 *The Nature of Mathematical Modeling* (Cambridge: Cambridge University Press)
[6] Burstedde C, Klauck K, Schadschneider A and Zittartz J, 2001 *Physica* A **295** 507
[7] Kirchner A and Schadschneider A, 2002 *Physica* A **312** 260
[8] Kirchner A, Nishinari K and Schadschneider A, 2003 *Phys. Rev.* E **67** 056122
[9] Gipps P G and Marksjö B, 1985 *Math. Comput. Simul.* **27** 95
[10] Blue V and Adler J, 1998 *Transp. Res. Rec.* **1644** 29
[11] Fukui M and Ishibashi Y, 1999 *J. Phys. Soc. Japan* **68** 2861
[12] Muramatsu M, Irie T and Nagatani T, 1999 *Physica* A **267** 487

[13] Klüpfel H, Meyer-König T, Wahle J and Schreckenberg M, 2000 *Proc. 4th Int. Conf. on Cellular Automata for Research and Industry* (London: Springer) pp 63–71
[14] Weidmann U, 1992 *Schriftenreihe des IVT* vol 90 (Zürich: ETH)
[15] 1994 *Special Report 209: Highway Capacity Manual* (Washington, DC: Transportation Research Board, National Research Council) chapter 13
[16] Kirchner A, Klüpfel H, Nishinari K, Schadschneider A and Schreckenberg M, 2003 *Physica* A **324** 689
[17] Chowdhury D, Santen L and Schadschneider A, 2000 *Phys. Rep.* **329** 199
[18] Schütz G M, *Exactly solvable models for many-body systems*, 2001 *Phase Transitions and Critical Phenomena* vol 19, ed C Domb and J L Lebowitz (New York: Academic)
[19] Evans M R and Blythe R A, 2002 *Physica* A **313** 110
[20] Ben-Jacob E, 1993 *Contemp. Phys.* **34** 247
[21] Chowdhury D, Guttal V, Nishinari K and Schadschneider A, 2002 *J. Phys. A: Math. Gen.* **35** L573
[22] Helbing D, Schweitzer F, Keltsch J and Molnar P, 1997 *Phys. Rev.* E **56** 2527
[23] Helbing D, Keltsch J and Molnar P, 1997 *Nature* **388** 47
[24] Kirchner A, 2002 *Dissertation* Universität zu Köln
[25] Klüpfel H, 2003 *Dissertation* Universität Duisburg (available from http://deposit.ddb.de/cgi-bin/dokserv?idn=96883180x)
[26] Helbing D and Molnar P, 1995 *Phys. Rev.* E **51** 4282
[27] Helbing D, Farkas I and Vicsek T, 2000 *Nature* **407** 487
[28] Wolf D E and Grassberger P (ed), 1997 *Friction, Arching, Contact Dynamics* (Singapore: World Scientific)
[29] Helbing D, 1991 *Behav. Sci.* **36** 298
[30] Thompson P and Marchant E, 1995 *Fire Safety J.* **24** 131
[31] Henderson L F, 1974 *Transp. Res.* **8** 509
[32] DiNenno P (ed), 1995 *SFPE Handbook of Fire Protection Engineering* 2nd edn (Quincy, MA: National Fire Protection Association)
[33] Helbing D, 1992 *Complex Syst.* **6** 391
[34] Hughes R, 2000 *Math. Comput. Simul.* **53** 367
[35] Hughes R, 2001 *Transp. Res.* B **36** 507
[36] Muir H, Bottomley D M and Marrison C, 1996 *Int. J. Aviat. Psychol.* **6** 57
[37] Helbing D, Buzna L and Werner T, *Self-organized pedestrian crowd dynamics and design solutions*, 2003 trafficforum/03120401 (available from www.trafficforum.org)
[38] Horlück S and Dimon P, 1999 *Phys. Rev.* E **60** 671
[39] Manna S S and Herrmann H J, 2000 *Eur. Phys. J.* **E1** 341
[40] Marconi S and Chopard B, 2002 *Cellular Automata* (*Lecture Notes in Computer Science* vol 2493) (Berlin, Heidelberg: Springer) p 231
[41] Maniccam S, 2003 *Physica* A **321** 653